Proceedings of the ASME 2011 International Mechanical Engineering Congress & Exposition
IMECE2011
November 11-17, 2011, Denver, Colorado, USA

IMECE2011-62694

MOTION PLANNING OF UNCERTAIN UNDER-ACTUATED DYNAMICAL SYSTEMS— A HYBRID DYNAMICS FORMULATION

Joe Hays
Mechanical Engineering
Virginia Tech
Blacksburg, VA 24061

Adrian Sandu
Computational Science Laboratory
Computer Science Department
Virginia Tech
Blacksburg, VA 24061

Corina Sandu
Advanced Vehicle Dynamics Laboratory
Mechanical Engineering
Virginia Tech
Blacksburg, VA 24061

Dennis Hong
Robotics and Mechanisms Laboratory
Mechanical Engineering
Virginia Tech
Blacksburg, VA 24061

Keywords: Motion Planning, Trajectory Planning, Optimization, Nonlinear Programming, Multibody Dynamics, Uncertainty Quantification, Under-Actuated Dynamical Systems

ABSTRACT

This work presents a novel nonlinear programming based motion planning framework that treats uncertain under-actuated dynamical systems described by ordinary differential equations. Uncertainty in multibody dynamical systems comes from various sources, such as: system parameters, initial conditions, sensor and actuator noise, and external forcing. Treatment of uncertainty in design is of paramount practical importance because all real-life systems are affected by it, and poor robustness and suboptimal performance result if it's not accounted for in a given design. System uncertainties are modeled using Generalized Polynomial Chaos and are solved quantitatively using a least-square collocation method. The computational efficiencies of this approach enable the inclusion of uncertainty statistics in the nonlinear programming optimization process. As such, new design questions related to uncertain dynamical systems can now be answered through the new framework.

Specifically, this work presents the new framework through a hybrid dynamics formulation for under-actuated systems where actuated state and unactuated input trajectories are prescribed and uncertain unactuated states and actuated inputs are quantified. The benefits of the ability to quantify the resulting uncertainties are illustrated in a power optimal motion planning case-study for an inverting double pendulum problem. The resulting design determines a motion plan that minimizes the required input power—subject to actuator and terminal condition variance constraints—for all possible systems within the probability space.

1 INTRODUCTION

Design engineers cannot quantify exactly every aspect of a given system. These uncertainties frequently create difficulties in accomplishing design goals and can lead to poor robustness and suboptimal performance. Tools that facilitate the analysis and characterization of the effects of uncertainties enable designers to develop more robustly performing systems. The need to analyze the effects of uncertainty is particularly acute when designing dynamical systems. Frequently, engineers do not account for various uncertainties in their design in order to save time and to reduce costs. However, this simply delays, or hides, the cost which is inevitably incurred down-stream in the design flow; or worse, after the system has been deployed and fails to meet the design goals. Ultimately, if a robust system design is to be achieved, uncertainties must be accounted for up-front during the design process.

This work presents a novel nonlinear programming (NLP) based motion planning framework that treats uncertain fully-actuated dynamical systems described by ordinary differential equations (ODEs). System uncertainties are modeled using Generalized Polynomial Chaos (gPC) and are solved quantitatively using a least-square collocation method (LSCM). The computational efficiencies gained by gPC and LSCM enable the inclusion of uncertainty statistics in the NLP optimization process.

Specifically, this work presents the new framework through a *hybrid dynamics* formulation for under-actuated systems where *actuated state* and *unactuated input* trajectories are prescribed and uncertain *unactuated states* and *actuated inputs* are quantified. The benefits of the ability to quantify the resulting uncertainties are illustrated in a *power optimal* motion planning case-study for an inverting double pendulum problem. The resulting design determines a motion plan that minimizes the required input power—subject to actuator and terminal condition variance constraints—for all possible systems within the probability space.

The companion formulations for fully-actuated systems based on uncertain inverse and forward dynamics are presented by the authors in [1, 2].

It's important to point out that the new framework is not dependent on the specific formulation of the equations of motion (EOMs); formulations such as, Newtonian, Lagrangian, Hamiltonian, and Geometric methodologies are all applicable. This work applies the analytical Lagrangian EOM formulation which is briefly introduced in Section 2; Section 3 briefly discusses the well studied deterministic motion planning problem with particular attention to the *hybrid dynamics* approach for under-actuated systems; Section 4 reviews the Generalized Polynomial Chaos methodology for uncertainty quantification when using *hybrid dynamics*; Section 5 introduces the new framework for motion planning of uncertain under-actuated dynamical systems based on the new *uncertain hybrid dynamics* formulation; finally, Section 6 illustrates the strengths of the new framework through a case-study of an inverting double pendulum followed by concluding remarks in Section 7.

2 UNDER-ACTUATED MULTIBODY DYNAMICS

As a very brief overview, the Euler-Lagrange ODE formulation for a multibody dynamical system can be described by [3, 4],

$$\begin{aligned} \boldsymbol{M}\big(\boldsymbol{q}(t),\boldsymbol{\theta}(t)\big)\dot{\boldsymbol{v}}(t) + \boldsymbol{C}\big(\boldsymbol{q}(t),\boldsymbol{v}(t),\boldsymbol{\theta}(t)\big)\boldsymbol{v}(t) \\ + \boldsymbol{N}\big(\boldsymbol{q}(t),\boldsymbol{v}(t),\boldsymbol{\theta}(t)\big) \\ = \boldsymbol{\mathcal{F}}\big(\boldsymbol{q}(t),\boldsymbol{v}(t),\dot{\boldsymbol{v}}(t),\boldsymbol{\theta}(t)\big) = \boldsymbol{\tau}(t) \end{aligned} \tag{1}$$

where $\boldsymbol{q}(t) \in \mathbb{R}^{n_d}$ are independent generalized coordinates equal in number to the number of degrees of freedom, n_d; $\boldsymbol{v}(t) \in \mathbb{R}^{n_d}$ the generalized velocities and—using Newton's *dot* notation—$\dot{\boldsymbol{v}}(t)$ contains their time derivatives; $\boldsymbol{\theta}(t) \in \mathbb{R}^{n_p}$ includes system parameters of interest; $M\big(\boldsymbol{q}(t),\boldsymbol{\theta}(t)\big) \in \mathbb{R}^{n_d \times n_d}$ is the square inertia matrix; $\boldsymbol{C}\big(\boldsymbol{q}(t),\boldsymbol{v}(t),\boldsymbol{\theta}(t)\big) \in \mathbb{R}^{n_d \times n_d}$ includes centrifugal, gyroscopic and Coriolis effects; $\boldsymbol{N}\big(\boldsymbol{q}(t),\boldsymbol{v}(t),\boldsymbol{\theta}(t)\big) \in \mathbb{R}^{n_d}$ represents the generalized gravitational and joint forces; and $\boldsymbol{\tau}(t) \in \mathbb{R}^{n_i}$ are the n_i applied inputs. (For notational brevity, all future equations will drop the explicit time dependence.)

The relationship between the time derivatives of the independent generalized coordinates and the generalized velocities is,

$$\dot{\boldsymbol{q}} = \boldsymbol{H}(\boldsymbol{q},\boldsymbol{\theta})\boldsymbol{v} \tag{2}$$

where $\boldsymbol{H}(\boldsymbol{q},\boldsymbol{\theta})$ is a skew-symmetric matrix that is a function of the selected kinematic representation (e.g., Euler Angles, Tait-Bryan angles, Axis-Angle, Euler Parameters, etc.) [5, 6]. However, if (1) is formulated with independent generalized coordinates and the system has a fixed base, as in [1, 2], then (2) becomes $\dot{\boldsymbol{q}} = \boldsymbol{v}$.

The trajectory of the system is determined by solving (1)–(2) as an initial value problem, where $\boldsymbol{q}(0) = \boldsymbol{q}_0$ and $\boldsymbol{v}(0) = \boldsymbol{v}_0$. Also, the system measured outputs are defined by,

$$\boldsymbol{y} = \boldsymbol{\mathcal{O}}(\boldsymbol{q},\dot{\boldsymbol{q}},\boldsymbol{\theta}) \tag{3}$$

where $\boldsymbol{y} \in \mathbb{R}^{n_o}$ with n_o equal to the number of outputs.

This work specifically treats under-actuated systems. An under-actuated system has at least one unactuated degree of freedom, or, $n_i < n_d$, where each actuated degree of freedom has one and only one associated actuator.

3 DETERMINISTIC MOTION PLANNING OF UNDER-ACTUATED SYSTEMS

The task of dynamic system motion planning is a well studied topic; it aims to determine a state, or input, trajectory to realize some prescribed objective. Sampled-based motion planning formulations, such as Rapid-exploring Random Trees (RRTs), primarily focus on finding a feasible solution [7-9]; where nonlinear programming formulations seek to determine at least a local optimal solution [10-27].

The under-actuated motion planning problem may be solved with a *forward dynamics* formulation, however, it is less efficient than the *hybrid dynamics* formulation presented here. Use of a *hybrid dynamics* formulation exploits the benefits of an *inverse dynamics* formulation for all actuated joints, ${}^{a}\boldsymbol{q}$, and relies on *forward dynamics* to solve the unactuated joints, ${}^{u}\boldsymbol{q}$. If state trajectories for actuated joints, $\{{}^{a}\boldsymbol{q}, {}^{a}\dot{\boldsymbol{q}}, {}^{a}\ddot{\boldsymbol{q}}\}$, are provided, then the *inverse dynamics* methodology can solve for the corresponding actuated inputs, or wrenches, ${}^{a}\boldsymbol{\tau}$, through a direct function evaluation. Likewise, if input wrench trajectories for the unactuated joints, ${}^{u}\boldsymbol{\tau}$, are provided then the *forward dynamics* methodology can solve for the corresponding unactuated positions and velocities by integrating ${}^{u}\dot{\boldsymbol{v}}$. This mixed methodology is frequently referred to as *hybrid dynamics* [12, 28]. Table 1 helps clarify the relations between known and unknown quantities,

Table 1—Hybrid Dynamics Knowns vs Unknowns

Joint Type	Known	Unknown
Actuated	${}^{a}\boldsymbol{q}$, ${}^{a}\dot{\boldsymbol{q}}$, ${}^{a}\ddot{\boldsymbol{q}}$, ${}^{a}\boldsymbol{v}$, ${}^{a}\dot{\boldsymbol{v}}$	${}^{a}\boldsymbol{\tau}$
Unactuated	${}^{u}\boldsymbol{\tau}$	${}^{u}\boldsymbol{q}$, ${}^{u}\dot{\boldsymbol{q}}$, ${}^{u}\ddot{\boldsymbol{q}}$, ${}^{u}\boldsymbol{v}$, ${}^{u}\dot{\boldsymbol{v}}$

where $\boldsymbol{\tau} = \{{}^{a}\boldsymbol{\tau}, {}^{u}\boldsymbol{\tau}\}$ and $\boldsymbol{q} = \{{}^{a}\boldsymbol{q}, {}^{u}\boldsymbol{q}\}$.

From a motion planning perspective, and following a similar approach as introduced by Sohl [15], ${}^{u}\boldsymbol{\tau}(\boldsymbol{P})$ and ${}^{a}\boldsymbol{q}(\boldsymbol{P})$ are parameterized with B-Splines to reduce the problem to a finite dimensional search, by,

$${}^{a}\boldsymbol{q}(\boldsymbol{P}),\ {}^{u}\boldsymbol{\tau}(\boldsymbol{P}) = \sum_{i=0}^{n_{sp}} \beta^{i,\mathcal{p}-1}(t)\boldsymbol{p}^{i} \tag{4}$$

where $\boldsymbol{p} \in \mathbb{R}^{n_d}$ are n_{sp} control points; β and $\mathcal{p}$ are the B-Splines' basis functions and degree, respectively; $\boldsymbol{P} \in \mathbb{R}^{n_{sp} \times n_d}$ is an vector of control points, $\boldsymbol{p}$. The parameterized rates and accelerations, ${}^{a}\dot{\boldsymbol{q}}(\boldsymbol{P})$ and ${}^{a}\ddot{\boldsymbol{q}}(\boldsymbol{P})$ are determined through direct derivation of ${}^{a}\boldsymbol{q}(\boldsymbol{P})$ resulting in lower order B-Splines [29]. Also, ${}^{a}\boldsymbol{v}(\boldsymbol{P})$ and ${}^{a}\dot{\boldsymbol{v}}(\boldsymbol{P})$ may be determined by differentiating (2) twice, yielding,

$$\ddot{\boldsymbol{q}}(\boldsymbol{P}) = \boldsymbol{H}(\boldsymbol{q}(\boldsymbol{P}),\boldsymbol{\theta})\dot{\boldsymbol{v}}(\boldsymbol{P}) + \boldsymbol{v}(\boldsymbol{P})\left(\frac{\partial \boldsymbol{H}}{\partial t} + \frac{\partial \boldsymbol{H}}{\partial \boldsymbol{q}}\frac{\partial \boldsymbol{q}}{\partial t} + \frac{\partial \boldsymbol{H}}{\partial \boldsymbol{\theta}}\frac{\partial \boldsymbol{\theta}}{\partial t}\right) \tag{5}$$

Solving (2) for $\boldsymbol{v}(\boldsymbol{P})$ and (5) for $\dot{\boldsymbol{v}}(\boldsymbol{P})$ yields,

$$\boldsymbol{v}(\boldsymbol{P}) = \big(\boldsymbol{H}(\boldsymbol{q}(\boldsymbol{P},t),\boldsymbol{\theta})\big)^{-1}\dot{\boldsymbol{q}}(\boldsymbol{P}) \tag{6}$$

$$\begin{aligned} \dot{\boldsymbol{v}}(\boldsymbol{P}) = \big(\boldsymbol{H}(\boldsymbol{q}(\boldsymbol{P}),\boldsymbol{\theta})\big)^{-1}\Bigg(\ddot{\boldsymbol{q}}(\boldsymbol{P}) \\ - \boldsymbol{v}(\boldsymbol{P},t)\left(\frac{\partial \boldsymbol{H}}{\partial t} + \frac{\partial \boldsymbol{H}}{\partial \boldsymbol{q}}\frac{\partial \boldsymbol{q}}{\partial t} + \frac{\partial \boldsymbol{H}}{\partial \boldsymbol{\theta}}\frac{\partial \boldsymbol{\theta}}{\partial t}\right)\Bigg) \end{aligned} \tag{7}$$

Once all known trajectories are parameterized the system of *hybrid dynamics* takes the form,

$$\begin{pmatrix} {}^{u}\dot{\boldsymbol{v}} \\ {}^{a}\boldsymbol{\tau} \end{pmatrix} = \boldsymbol{\mathcal{G}}({}^{a}\boldsymbol{q}(\boldsymbol{P}),\ {}^{a}\boldsymbol{v}(\boldsymbol{P}),\ {}^{a}\dot{\boldsymbol{v}}(\boldsymbol{P}),\ {}^{u}\boldsymbol{\tau}(\boldsymbol{P}),\boldsymbol{\theta}) \tag{8}$$

It is worth mentioning that the unactuated input wrenches, ${}^{u}\boldsymbol{\tau}$, represent joint constraint forces. Depending on the formulation used to determine the EOMS then ${}^{u}\boldsymbol{\tau}$ may be implicitly known once $\{{}^{a}\boldsymbol{q}(\boldsymbol{P}), {}^{a}\boldsymbol{v}(\boldsymbol{P}), {}^{a}\dot{\boldsymbol{v}}(\boldsymbol{P})\}$ are specified. In such a formulation (8) reduces to,

$$\begin{pmatrix} {}^{u}\dot{\boldsymbol{v}} \\ {}^{a}\boldsymbol{\tau} \end{pmatrix} = \boldsymbol{\mathcal{G}}({}^{a}\boldsymbol{q}(\boldsymbol{P}),\ {}^{a}\boldsymbol{v}(\boldsymbol{P}),\ {}^{a}\dot{\boldsymbol{v}}(\boldsymbol{P}), \boldsymbol{\theta}) \tag{9}$$

Once (8) or (9) is determined then the NLP-based deterministic motion planning problem may be formulated as,

$$\begin{aligned}
&\min_{x=\{\boldsymbol{P}\}} && \mathrm{J} \\
&\text{s. t.} && \textbf{Actuated kinematics} \\
&&& {}^{a}\boldsymbol{v}(\boldsymbol{P}) = \left(\boldsymbol{H}({}^{a}\boldsymbol{q}(\boldsymbol{P}), \boldsymbol{\theta})\right)^{-1}\ {}^{a}\dot{\boldsymbol{q}}(\boldsymbol{P}) \\
&&& {}^{a}\dot{\boldsymbol{v}}(\boldsymbol{P}) = \left(\boldsymbol{H}({}^{a}\boldsymbol{q}(\boldsymbol{P}), \boldsymbol{\theta})\right)^{-1} * \\
&&&\qquad \left({}^{a}\ddot{\boldsymbol{q}}(\boldsymbol{P}) - {}^{a}\boldsymbol{v}(\boldsymbol{P})\left(\frac{\partial \boldsymbol{H}}{\partial t} + \frac{\partial \boldsymbol{H}}{\partial \boldsymbol{q}}\frac{\partial \boldsymbol{q}}{\partial t} + \frac{\partial \boldsymbol{H}}{\partial \boldsymbol{\theta}}\frac{\partial \boldsymbol{\theta}}{\partial t}\right)\right) \\
&&& \textbf{Hybrid dynamics} \\
&&& \begin{pmatrix} {}^{u}\dot{\boldsymbol{v}} \\ {}^{a}\boldsymbol{\tau} \end{pmatrix} = \boldsymbol{\mathcal{G}}({}^{a}\boldsymbol{q}(\boldsymbol{P}),\ {}^{a}\boldsymbol{v}(\boldsymbol{P}),\ {}^{a}\dot{\boldsymbol{v}}(\boldsymbol{P}),\ {}^{u}\boldsymbol{\tau}(\boldsymbol{P}), \boldsymbol{\theta}) \\
&&& \textbf{Unactuated kinematics} \\
&&& {}^{u}\dot{\boldsymbol{q}} = {}^{u}\boldsymbol{H}({}^{u}\boldsymbol{q}, \boldsymbol{\theta})\ {}^{u}\boldsymbol{v} \\
&&& \textbf{Outputs} \\
&&& \boldsymbol{y} = \boldsymbol{O}(\boldsymbol{q}(\boldsymbol{P}), \dot{\boldsymbol{q}}(\boldsymbol{P}), \boldsymbol{\theta}) \\
&&& \textbf{Constraints} \\
&&& \boldsymbol{\mathcal{C}}(\boldsymbol{y}, \boldsymbol{\tau}, \boldsymbol{\theta}) \leq \boldsymbol{0} \\
&&& \textit{Hard}\textbf{ actuated ICs \& TCs} \\
&&& {}^{a}\boldsymbol{q}(0) = {}^{a}\boldsymbol{P}^{0} = {}^{a}\boldsymbol{q}_{0} \\
&&& {}^{a}\dot{\boldsymbol{q}}(0) = {}^{a}\boldsymbol{P}^{0} = {}^{a}\dot{\boldsymbol{q}}_{0} \\
&&& {}^{a}\boldsymbol{q}(t_f) = {}^{a}\boldsymbol{P}^{n_{sp}} = {}^{a}\boldsymbol{q}_{t_f} \\
&&& {}^{a}\dot{\boldsymbol{q}}(t_f) = {}^{a}\boldsymbol{P}^{n_{sp}-1} = {}^{a}\dot{\boldsymbol{q}}_{t_f} \\
&&& \textit{Hard}\textbf{ unactuated ICs \& TCs} \\
&&& {}^{u}\boldsymbol{q}(0) = {}^{u}\boldsymbol{q}_{0} \\
&&& {}^{u}\dot{\boldsymbol{q}}(0) = {}^{u}\dot{\boldsymbol{q}}_{0} \\
&&& {}^{u}\boldsymbol{q}(t_f) = {}^{u}\boldsymbol{q}_{t_f} \\
&&& {}^{u}\dot{\boldsymbol{q}}(t_f) = {}^{u}\dot{\boldsymbol{q}}_{t_f}
\end{aligned} \tag{10}$$

Equation (10) seeks to find the control points $\boldsymbol{P}$ that minimizes some prescribed objective function, J, while being subject to the *hybrid dynamic* constraints defined in (8). Notice how the kinematic equations defined in (5)–(7) have been require being split between actuated and unactuated variants, where the actuated kinematic equations are evaluated before the dynamics (8). After the dynamics are evaluated then the unactuated kinematics may be determined. Additional constraints may also be defined; for example, maximum/minimum actuator and system parameter limits or physical system geometric limits can be represented as inequality relations, $\boldsymbol{\mathcal{C}}(\boldsymbol{y}, \boldsymbol{\tau}, \boldsymbol{\theta}) \leq \boldsymbol{0}$. Equation (10) explicitly differentiates between the initial conditions (ICs) and terminal conditions (TCs) for the actuated and unactuated states. All actuated ICs and TCs are determined by corresponding control points in, $\boldsymbol{P}$, where all unactuated ICs and TCs are freely defined. When ICS and/or TCs are explicitly defined as shown in (10) they are referred to as *hard* constraints; conversely, if the constraints are added to the definition of the objective function, J, then they are refered to as *soft* constraints.

In [1] the authors itemized common motion planning objective function definitions from the literature; the *power optimal* objective function, used in the accompanying case study, is repeat for convenience ,

$$\mathrm{J} = \sum_{i=1}^{n_i} |\tau_i \dot{q}_i|, \quad \forall t \tag{11}$$

The solution to (10) produces an optimal motion plan under the assumption that all system properties are known (i.e., (1) is completely deterministic). The primary contribution of this work is the presentation of a variant of (10) that allows (1) to contain uncertainties of diverse types (e.g., parameters, initial conditions, sensor/actuator noise, or forcing functions). The following section will briefly introduce Generalized Polynomial Chaos (gPC) which is used to model the uncertainties and to quantify the resulting uncertain system states and inputs.

4 GENERALIZED POLYNOMIAL CHAOS

Generalized Polynomial Chaos (gPC), first introduced by Wiener [30], is an efficient method for analyzing the effects of uncertainties in second order random processes [31]. This is accomplished by approximating a source of uncertainty, θ, with an infinite series of weighted orthogonal polynomial bases called Polynomial Chaoses. Clearly an infinite series is impractical; therefore, a truncated set of $p_o + 1$ terms is used with $p_o \in \mathbb{N}$ representing the *order* of the approximation. Or,

$$\theta(\xi) = \sum_{j=0}^{p_o} \theta^j \psi^j\left(\xi(\omega)\right) \tag{12}$$

where $\theta^j \in \mathbb{R}$ represent known stochastic coefficients; $\psi^j \in \mathbb{R}$ represent individual single dimensional orthogonal basis terms (or modes); $\xi(\omega) \in \mathbb{R}$ is the associated random variable for θ that maps the random event $\omega \in \Omega$, from the sample space, Ω, to the domain of the orthogonal polynomial basis (e.g., $\xi: \Omega \to [-1,1]$).

Polynomial chaoses are orthogonal with respect to the ensemble inner product,

$$\langle \psi^i(\xi), \psi^j(\xi) \rangle = \int_{-1}^{1} \psi^i(\xi)\psi^j(\xi) w(\xi) d\xi = 0, \quad \text{for i}\neq\text{j} \tag{13}$$

where $w(\xi)$ is the weighting function that is equal to the joint probability density function of the random variable ξ. Also, $\langle \Psi^j, \Psi^j \rangle = 1, \forall j$ when using *normalized basis*; *standardized basis* are constant and may be computed off-line for efficiency using (13).

gPC can be applied to multibody dynamical systems described by differential equations [32, 33]. The presence of uncertainty in the system results in uncertain states and inputs, in the case of a *hybrid dynamics* formulation. Therefore, the uncertain states/inputs can be approximated in a similar fashion as (12),

$${}^{u}\dot{v}_i(\xi; t) = \sum_{j=0}^{n_b} {}^{u}\dot{v}_i^j(t)\Psi^j(\xi), \qquad i = 1 \ldots {}^{u}n_s \tag{14}$$

$${}^{a}\tau_i(\xi; t) = \sum_{j=0}^{n_b} {}^{a}\tau_i^j(t)\Psi^j(\xi), \qquad i = 1 \ldots {}^{a}n_i \tag{15}$$

where ${}^{u}\dot{v}_i^j(t) \in \mathbb{R}^{n_b}$ represent the stochastic coefficients for the i^{th} state; ${}^{a}\tau_i^j(t) \in \mathbb{R}^{n_b}$ represent the stochastic coefficients for the i^{th} input; $n_b \in \mathbb{N}$ representing the number of basis terms in the approximation. Notice how these stochastic coefficients are unknown functions of time.

The stochastic basis may be multidimensional in the event there are multiple sources of uncertainty. The multidimensional basis functions are represented by $\Psi^j \in \mathbb{R}^{n_b}$. Additionally, $\boldsymbol{\xi}$ becomes a vector of random variables, $\boldsymbol{\xi} = \{\xi_1, \ldots, \xi_{n_p}\} \in \mathbb{R}^{n_p}$ and maps the sample space, Ω, to an n_p dimensional cuboid, $\boldsymbol{\xi}: \Omega \to [-1,1]^{n_p}$ (as in the example of Jacobi chaoses).

The multidimensional basis is constructed from a product of the single dimensional basis in the following manner,

$$\Psi^j = \psi_1^{i_1}\psi_2^{i_2} \ldots \psi_{n_p}^{i_{n_p}}, \quad i_k = 0 \ldots p_o, k = 1 \ldots n_p \tag{16}$$

where subscripts represent the uncertainty source and superscripts represent the associated basis term (or mode). A complete set of basis

may be determined from a full tensor product of the single dimensional bases. This results in an excessive set of $(p_o+1)^{n_p}$ basis terms. Fortunately, the multidimensional sample space can be spanned with a minimal set of $n_b = \frac{(n_p+p_o)!}{n_p!\,p_o!}$ basis terms. The minimal basis set can be determined by the products resulting from these index ranges,

$$i_1 = 0 \dots p_o,$$
$$i_2 = 0 \dots (p_o - i_1), \dots,$$
$$i_{n_p} = 0 \dots \left(p_o - i_1 - i_2 - \cdots - i_{(n_p-1)}\right)$$

The number of multidimensional terms, n_b, grows quickly with the number of uncertain parameters, n_p, and polynomial order, p_o. Sandu, Sandu, and Ahmadian showed that gPC is most appropriate for modeling systems with a relatively low number of uncertainties [32, 33] but can handle large nonlinear uncertainty magnitudes.

Substituting (12) and (14)–(15) into (8) produces the following *uncertain hybrid dynamics* (UHD),

$$\begin{pmatrix} \sum_{j=0}^{n_b} {}^{u}\dot{v}_i^j(t)\Psi^j(\xi) \\ \sum_{j=0}^{n_b} {}^{a}\tau_l^j(t)\Psi^j(\xi) \end{pmatrix} = \boldsymbol{\mathcal{G}}\left({}^{\boldsymbol{a}}\boldsymbol{q}(\boldsymbol{P}),\ {}^{\boldsymbol{a}}\boldsymbol{v}(\boldsymbol{P}),\ {}^{\boldsymbol{a}}\dot{\boldsymbol{v}}(\boldsymbol{P}),\ {}^{\boldsymbol{u}}\boldsymbol{\tau}(\boldsymbol{P}), \sum_{j=0}^{p_o}\theta^j\psi^j(\xi) \right), \quad i = 1 \dots {}^{u}n_s, l = 1 \dots {}^{a}n_i \tag{17}$$

where the unknowns are now the $n_b\,{}^{u}n_s$ unactuated uncertain state coefficients, ${}^{u}\dot{v}_i^j$, and the $n_b\,{}^{a}n_i$ actuated uncertain input coefficients. Revisiting Table 1, all unknown quantities become uncertain in the *uncertain hybrid dynamics* formulation.

It is instructive to notice how time and randomness are decoupled within a single term after the gPC expansion. Only the stochastic coefficients are dependent on time, and only the basis terms are dependent on the n_b random variables, $\boldsymbol{\xi}$.

The Galerkin Projection Method (GPM) is a commonly used method for solving (17), however, this is a very intrusive technique and requires a custom formulation of the *hybrid dynamic* EOMs. As an alternative, sample-based collocation techniques can be used without the need to modify the base EOMs.

Reference [32] showed that the collocation method solves (17) by solving (1)–(3) at a set of points, ${}_k\boldsymbol{\mu} \in \mathbb{R}^{n_p},\ k = 1 \dots n_{cp}$, selected from the n_p dimensional domain of the random variables $\boldsymbol{\xi} \in \mathbb{R}^{n_p}$. Meaning, at any given instance in time, the random variables' domain is sampled and solved n_{cp} times with $\boldsymbol{\xi} = {}_k\boldsymbol{\mu}$ (updating the approximations of all sources of uncertainty for each solve), then the uncertain coefficients can be determined at that given time instance. This can be accomplished by defining the intermediate variables,

$${}^{u}_{k}\dot{V}_i(t;\ {}_k\boldsymbol{\mu}) = \sum_{j=0}^{n_b}\dot{v}_i^j(t)\Psi^j({}_k\boldsymbol{\mu}),\ \ i = 1 \dots {}^{u}n_s, k = 0 \dots n_{cp} \tag{18}$$

$${}^{a}_{k}T_l(t;\ {}_k\boldsymbol{\mu}) = \sum_{j=0}^{n_b}\tau_l^j(t)\Psi^j({}_k\boldsymbol{\mu}),\ \ l = 1 \dots {}^{a}n_i, k = 0 \dots n_{cp} \tag{19}$$

and substituting them into (17). This yields,

$$\begin{pmatrix} {}^{u}_{k}\dot{V}_i(t;\ {}_k\boldsymbol{\mu}) \\ {}^{a}_{k}T_l(t;\ {}_k\boldsymbol{\mu}) \end{pmatrix} = \mathcal{G}\left({}^{\boldsymbol{a}}\boldsymbol{q},\ {}^{\boldsymbol{a}}\boldsymbol{v},\ {}^{\boldsymbol{a}}\dot{\boldsymbol{v}},\ {}^{\boldsymbol{u}}\boldsymbol{\tau},\ {}_k\Theta_r(t;\ {}_k\boldsymbol{\mu})\right), \quad i = 1 \dots {}^{u}n_s, l = 1 \dots {}^{a}n_i, r = 1 \dots n_p, k = 0 \dots n_{cp} \tag{20}$$

where,

$${}_k\Theta_r(t;\ {}_k\boldsymbol{\mu}) = \sum_{j=0}^{p_o}\theta_r^j(t)\,\psi^j({}_k\boldsymbol{\mu}),\ \ k = 0 \dots n_{cp}, r = 1 \dots n_p \tag{21}$$

Equation (20) provides a set of n_{cp} independent equations whose solutions determine the uncertain stochastic coefficients, $\{\mathrm{q}_i^j, v_i^j\ \dot{v}_i^j, \tau_l^j\}$. This is accomplished by recalling the relationship of the stochastic coefficients to the solutions, ${}_k\dot{V}_i$, shown in (18)–(19). In matrix notation (18)–(19) can be expressed for all states,

$$\dot{\boldsymbol{V}}_i = \left(\dot{\boldsymbol{v}}_i(t)\right)^{\boldsymbol{T}}\boldsymbol{\Psi}(\boldsymbol{\mu}), \qquad i = 1 \dots {}^{u}n_s \tag{22}$$

$$\boldsymbol{T}_l = \left(\boldsymbol{\tau}_l(t)\right)^{\boldsymbol{T}}\boldsymbol{\Psi}(\boldsymbol{\mu}), \qquad l = 1 \dots {}^{a}n_i \tag{23}$$

where the matrix,

$$A_{k,j} = \Psi^j\left({}_k\mu\right),\ \ j = 0 \dots n_b, k = 0 \dots n_{cp} \tag{24}$$

is defined as the *collocation matrix*. It's important to note that $n_b \le n_{cp}$. The stochastic coefficients can now be solved for using (22)–(23),

$$\dot{v}_i^j(t) = \boldsymbol{A}^{\#}\dot{\boldsymbol{V}}_i, \qquad i = 1 \dots {}^{u}n_s, j = 0 \dots n_b \tag{25}$$

$$\tau_l^j(t) = \boldsymbol{A}^{\#}\boldsymbol{T}_l, \qquad l = 1 \dots {}^{a}n_i, j = 0 \dots n_b \tag{26}$$

where $A^{\#}$ is the pseudo inverse of A if $n_b < n_{cp}$. If $n_b = n_{cp}$, then (25)–(26) are simply a linear solve. However, [34] presented the least-squares collocation method (LSCM) where the stochastic state coefficients are solved for, in a least squares sense, using (25)–(26) when $n_b < n_{cp}$. Reference [34] also showed that as $n_{cp} \to \infty$ the LSCM approaches the GPM solution; where by selecting $3n_b \le n_{cp} \le 4n_b$ the greatest convergence benefit is achieved with minimal computational cost. LSCM also enjoys the same exponential convergence rate as $p_o \to \infty$.

The unintrusive nature of the LSCM sampling approach is arguably its greatest benefit; (8) may be repeatedly solved without modification. Also, there are a number of methods for selecting the collocation points and the interested reader is recommended to consult [32, 34-37] for more information.

5 UNCERTAIN HYBRID DYNAMICS MOTION PLANNING

Little work is found in the literature addressing motion planning for uncertain systems. The literature thus far has primarily addressed sensor and/or actuator noise [7, 38] and frequently only treats the system's kinematics [39, 40].

In [41], Kewlani presents an RRT planner for mobility of robotic systems based on gPC but refers to it as a stochastic response surface method (SRSM). Kewlani's work is similar in spirit to this work, however, the main difference is Kewlani's solution is developed only for determining a feasible motion plan. The motion planning framework of this paper is formulated within a NLP setting and thus benefits from the more efficient gradient-based searching techniques providing at least a locally optimal design.

As such, the new NLP-based framework for motion planning of uncertain under-actuated multibody dynamical systems, formulated with *uncertain hybrid dynamics*, is,

$$\min_{\boldsymbol{x}=\{\boldsymbol{P}\}}\ \mathrm{J}$$

s.t.

Actuated kinematics

$$\begin{aligned} {}^{\boldsymbol{a}}\boldsymbol{v}(\boldsymbol{P}) &= \left(\boldsymbol{H}({}^{\boldsymbol{a}}\boldsymbol{q}(\boldsymbol{P}), \boldsymbol{\theta})\right)^{-1}\ {}^{\boldsymbol{a}}\dot{\boldsymbol{q}}(\boldsymbol{P}) \\ {}^{\boldsymbol{a}}\dot{\boldsymbol{v}}(\boldsymbol{P}) &= \left(\boldsymbol{H}({}^{\boldsymbol{a}}\boldsymbol{q}(\boldsymbol{P}), \boldsymbol{\theta})\right)^{-1} * \\ &\qquad \left({}^{\boldsymbol{a}}\ddot{\boldsymbol{q}}(\boldsymbol{P}) - {}^{\boldsymbol{a}}\boldsymbol{v}(\boldsymbol{P})\left(\frac{\partial \boldsymbol{H}}{\partial t} + \frac{\partial \boldsymbol{H}}{\partial \boldsymbol{q}}\frac{\partial \boldsymbol{q}}{\partial t} + \frac{\partial \boldsymbol{H}}{\partial \boldsymbol{\theta}}\frac{\partial \boldsymbol{\theta}}{\partial t}\right)\right) \end{aligned} \tag{27}$$

Uncertain hybrid dynamics

$$\begin{pmatrix} {}^{\boldsymbol{u}}\dot{\boldsymbol{v}}(t;\boldsymbol{\xi}) \\ {}^{\boldsymbol{a}}\boldsymbol{\tau}(t;\boldsymbol{\xi}) \end{pmatrix} = \boldsymbol{\mathcal{G}}({}^{\boldsymbol{a}}\boldsymbol{q}(\boldsymbol{P}),\ {}^{\boldsymbol{a}}\boldsymbol{v}(\boldsymbol{P}),\ {}^{\boldsymbol{a}}\dot{\boldsymbol{v}}(\boldsymbol{P}),\ {}^{\boldsymbol{u}}\boldsymbol{\tau}(\boldsymbol{P}), \boldsymbol{\theta}(\boldsymbol{\xi}))$$

Uncertain unactuated kinematics

$$
\begin{aligned}
&{}^{u}\dot{\boldsymbol{q}}(\xi) = {}^{u}\boldsymbol{H}\left({}^{u}\boldsymbol{q}(\xi), \boldsymbol{\theta}(\xi)\right) {}^{u}\boldsymbol{v}(\xi) \\
&\textit{Uncertain outputs} \\
&\boldsymbol{y}(\xi) = \boldsymbol{\mathcal{O}}\big(\boldsymbol{q}(\boldsymbol{P};\xi), \dot{\boldsymbol{q}}(\boldsymbol{P};\xi), \boldsymbol{\theta}(\xi)\big) \\
&\textit{Uncertain constraints} \\
&\boldsymbol{\mathcal{C}}(\boldsymbol{y}(\xi), \boldsymbol{\theta}(\xi), \boldsymbol{\tau}(\xi)) \leq \boldsymbol{0} \\
&\textit{Hard}\text{ actuated ICs \& TCs} \\
&{}^{a}\boldsymbol{q}(0) = {}^{a}\boldsymbol{P}^{0} = {}^{a}\boldsymbol{q}_{0} \\
&{}^{a}\dot{\boldsymbol{q}}(0) = {}^{a}\boldsymbol{P}^{0} = {}^{a}\dot{\boldsymbol{q}}_{0} \\
&{}^{a}\boldsymbol{q}(t_f) = {}^{a}\boldsymbol{P}^{n_{sp}} = {}^{a}\boldsymbol{q}_{t_f} \\
&{}^{a}\dot{\boldsymbol{q}}(t_f) = {}^{a}\boldsymbol{P}^{n_{sp}-1} = {}^{a}\dot{\boldsymbol{q}}_{t_f} \\
&\textit{Hard}\text{ uncertain unactuated ICs \& TCs} \\
&{}^{u}\boldsymbol{q}(0;\xi) = {}^{u}\boldsymbol{q}_{0}(\xi) \\
&{}^{u}\dot{\boldsymbol{q}}(0;\xi) = {}^{u}\dot{\boldsymbol{q}}_{0}(\xi) \\
&{}^{u}\boldsymbol{q}(t_f;\xi) = {}^{u}\boldsymbol{q}_{t_f}(\xi) \\
&{}^{u}\dot{\boldsymbol{q}}(t_f;\xi) = {}^{u}\dot{\boldsymbol{q}}_{t_f}(\xi)
\end{aligned}
$$

where (27) is a reformulation of (10) using the *uncertain hybrid dynamics* defined in (17) with uncertain actuated inputs and unactuated states. The most interesting part of (27) comes in the definition of the objective function terms and constraints. These terms now have the ability to approach the design accounting for uncertainties by way of expected values, variances, and standard deviations. In the *uncertain hybrid dynamics* formulation, the actuated state and unactuated input profiles are deterministic. Therefore, the objective function for *time optimal*, *effort optimal*, and *jerk optimal* (as presented in [1]) are deterministically defined. However, a *power optimal* design would necessitate statistical objective functions of the form,

$$
\begin{aligned}
\mathrm{J}_{\mathrm{S1}} &= E\left[\sum_{i=1}^{n_i} \left|\mathrm{z}_i \tau_i(\xi) \mathrm{y}_i(\xi)\right|\right] \\
&= \textstyle\sum_{i=1}^{n_i} \sum_{j=0}^{n_b} \left|\mathrm{z}_i \tau_i^j \mathrm{y}_i^j \langle \Psi^j, \Psi^j \rangle\right|, \ \forall t
\end{aligned}
\tag{28}
$$

where z_i are optional scalarization weights; (28) is the expected power profile.

Designs may necessitate statistically penalizing terminal conditions (TC) of the state or output trajectories in the objective function (occasionally referred to as *soft* constraints). Two candidates are,

$$
\begin{aligned}
\mathrm{J}_{\mathrm{S2}} &= \left\|\mu_{e(t_f)}\right\| = \left\|E\left[\boldsymbol{e}(t_f;\xi)\right]\right\| \\
&= \left\|\boldsymbol{y}_{ref}(t_f) - \boldsymbol{y}^0(t_f)\langle \Psi^0, \Psi^0 \rangle\right\|
\end{aligned}
\tag{29}
$$

$$
\begin{aligned}
\mathrm{J}_{\mathrm{S3}} &= \left\|\sigma^2_{e(t_f)}\right\| \\
&= \left\|E\left[\left(\boldsymbol{e}(\mathrm{t_f};\xi) - \mu_{e(t_f)}\right)^2\right]\right\| \\
&= \left\|\textstyle\sum_{j=0}^{n_b} \left(\boldsymbol{y}^j(\mathrm{t_f})\right)^2 \langle \Psi^j, \Psi^j \rangle\right\|
\end{aligned}
\tag{30}
$$

where $\boldsymbol{e}(\mathrm{t_f};\xi) = \boldsymbol{y}_{ref}(\mathrm{t_f}) - \boldsymbol{y}(\mathrm{t_f};\xi)$; (29) is the expected value of the TC's error; (30) is the corresponding variance of the TC's error. Notice that due to the orthogonality of the polynomial basis these computations result in a reduced set of efficient operations on the respective stochastic coefficients.

The inequality constraints may also benefit from added statistical information; for example, bounding the expected values can be expressed as,

$$
\boldsymbol{\mathcal{C}}(t;\xi) = \underline{\boldsymbol{y}} \leq E[\boldsymbol{y}(\xi)] \leq \overline{\boldsymbol{y}} \tag{31}
$$

where $E[\boldsymbol{y}(\xi)] = \mu_{\boldsymbol{y}} = \boldsymbol{y}^0\langle \Psi^j, \Psi^j \rangle$, and $\left\{\underline{\boldsymbol{y}}, \overline{\boldsymbol{y}}\right\}$ are the minimum/maximum output bounds respectively.

Collision avoidance constraints would ideally involve *supremum* and *infimum* bounds,

$$
\underline{\boldsymbol{y}} \leq \inf\big(\boldsymbol{y}(t;\xi)\big), \ \ \sup\big(\boldsymbol{y}(t;\xi)\big) \leq \overline{\boldsymbol{y}} \tag{32}
$$

However, one major difficulty with *supremum* and *infimum* bounds is that they are expensive to calculate. An alternative can be to constrain the uncertain configuration in a standard deviation sense; collision constraints would then take the form,

$$
\begin{aligned}
\mu_{\boldsymbol{y}} + \sigma_{\boldsymbol{y}} &\leq \overline{\boldsymbol{y}} \\
\underline{\boldsymbol{y}} &\leq \mu_{\boldsymbol{y}} - \sigma_{\boldsymbol{y}}
\end{aligned}
\tag{33}
$$

where $stddev[\boldsymbol{y}(\xi)] = \sigma_{\boldsymbol{y}} = \sqrt{\sum_{j=1}^{n_b} \mathbf{y}^{\mathrm{j}} \langle \Psi^j, \Psi^j \rangle}$.

6 AN INVERTING DOUBLE PENDULUM CASE-STUDY

As an illustration of (27), an inverting double pendulum problem will be used, as seen in Figure 1. The design objective is to minimize the power it takes to move the manipulator from its initial hanging configuration, $\boldsymbol{q}_0$, to the target inverted configuration, $\boldsymbol{q}_{t_f}$. The double pendulum is an under-actuated system, where only joint q_1 is actuated (by input wrench τ_1), and the mass of the second link is uncertain, therefore, the motion planning problem may be appropriately defined by (27).

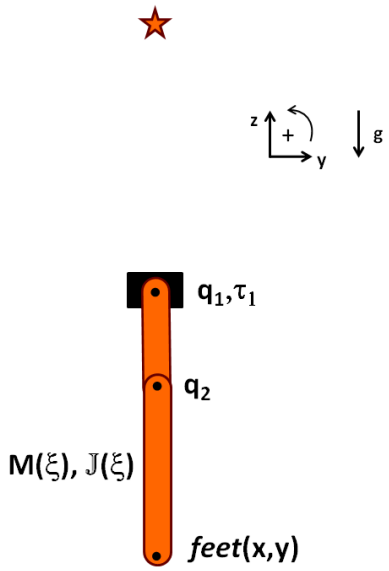

Figure 1—A simple illustration of the under-actuated *uncertain hybrid dynamics* motion planning formulation; this problem aims to determine a *power optimal* motion plan subject to input wrench and terminal condition constraints. This is an uncertain system due to the uncertain mass of the payload.

By parameterizing the actuated state profiles with B-Splines, as in (4), and using the *hybrid dynamics* defined in (9), (27) results in a finite search problem seeking for spline control points, **P**, and terminal time, t_f, that minimize the system's power. Therefore, the problem's optimization variables are $\boldsymbol{x} = \{\mathbf{P}, t_f\}$. Assuming a *soft* terminal error expected value condition is used, the objective function becomes $J = a \cdot \mathrm{J}_{\mathrm{S1}} + b \cdot \mathrm{J}_{\mathrm{S2}}$ from (28)–(29); where a and b are scalarization constants.

The actuators are bounded in their torque supply. Additionally, suppose the design has a specified variance in the terminal error conditions (30) that must be satisfied. Implementing both of these design constraints as *hard* constraints takes the form,

$$\mathcal{C}: \begin{cases} \underline{\tau} \le \tau \le \bar{\tau} \\ \sigma^2_{e(t_f)} \le \bar{\sigma}^2_{e(t_f)} \end{cases} \quad (34)$$

where $\{\underline{\tau}, \bar{\tau}\}$ are the minimum/maximum input bounds respectively; $\bar{\sigma}^2_{e(t_f)}$ is the maximum terminal error variance.

This formulation allows a design engineer to answer the question,

> *Given actuator and terminal error variance constraints, what motion plan will minimize the system's power over the trajectory when accounting for all possible systems within the probability space?*

Without accounting for the uncertainty directly in the dynamics and motion planning formulations, design engineers would have a difficult time answering this question. As a result, manufacturing lines, or other applicable applications, would result in reduced yield rates potentially affecting a company's financial *bottom-line*.

The solution to this problem with the deterministic formulation, as defined in (10), results in an *power optimal* solution of $J_{S1} = 1060\ (W)$ with $t_f = 5.66$ seconds; all system parameters are set equal to one, $\theta_i = 1$ (with SI units) except the length of the first link is set to 0.5 (m); initial conditions $\boldsymbol{q}(0) = \{-\pi, 0\}$ and $\dot{\boldsymbol{q}}(0) = \{0, 0\}$ radians; terminal conditions $\boldsymbol{q}(t_f) = \{0, 0\}$ and $\dot{\boldsymbol{q}}(t_f) = \{0, 0\}$ radians; and the input limits are $\underline{\tau} = -10, \bar{\tau} = 10\ (N \cdot m)$. The resulting optimal motion plan's configuration time history is shown in Figure 2.

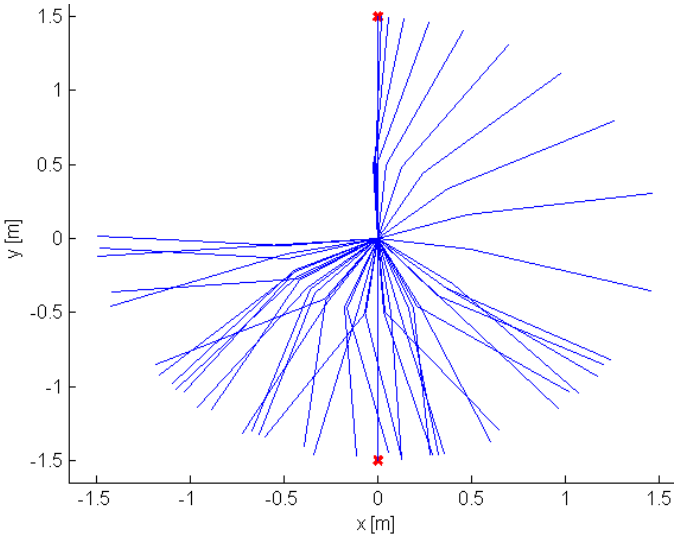

Figure 2—The *power optimal* configuration time history for the deterministic inverting double pendulum. This optimal solution resulted in a 1060 (W) design.

The value of the new framework is best illustrated by applying the deterministically designed motion profile to an uncertain system. Figure 3 and Figure 4 show the results of the deterministic motion plan applied to a system with a single uncertainty; the second link has an uncertain mass with $\mu_{m2} = 1\ (kg)$ and $\sigma^2_{m2} = 0.5\ (kg^2)$. Figure 3 shows that the resulting input wrench profile exceeds both the upper and lower bounding constraints of $\underline{\tau} = -10, \bar{\tau} = 10\ \ (N \cdot m)$. Additionally, Figure 4 shows that the target terminal configuration was not satisfied and an excessive terminal error variance is experienced.

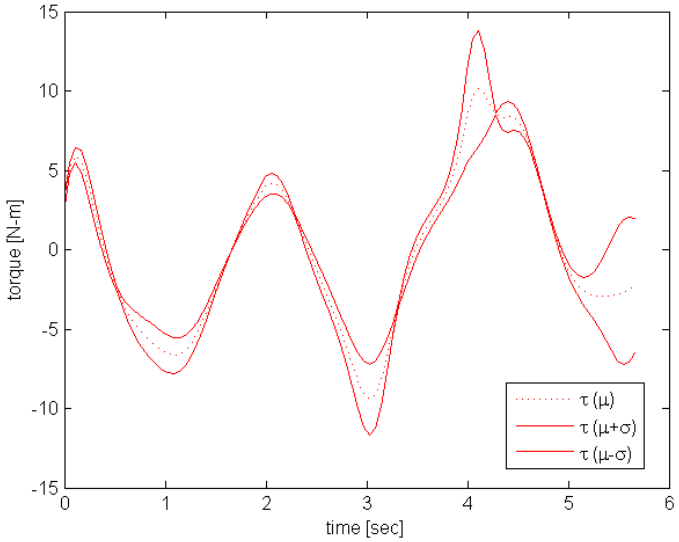

Figure 3—The uncertain input wrench time history for the deterministically design motion plan applied to an uncertain inverting double pendulum. The presence of the uncertainty results in both the maximum and minimum input limits being exceeded.

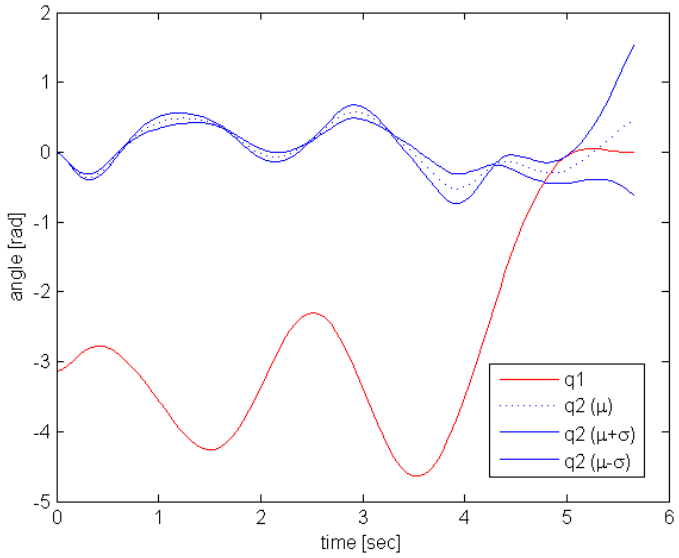

Figure 4—The joint time histories for the deterministically design motion plan applied to an uncertain inverting double pendulum. The presence of the uncertainty results in the expected terminal error condition not being satisfied with excessive variance.

Approaching the design with the new framework accounts for the uncertainties up front during the optimal search and results in a design that satisfies all constraints for all possible systems in the probability space. This is accomplished by application of (27) with constraints defined by (34); where $\bar{\sigma}^2_{e(t_f)} = 0.01\ (m^2)$. This results in a *power optimal* solution of $J_{S1} = 310\ (W)$ with $t_f = 4.46$ seconds; where the same uncertain second link mass is reused. The resulting motion plan's optimal uncertain configuration time history is illustrated in Figure 5; where the bounding $\{\mu_y - \sigma_y\ (red),\ \mu_y + \sigma_y\ (blue)\}$ configuration time histories are displayed. The Euclidean norm of the *soft* expected value terminal configuration constraint was very acceptable,

$\|E[\boldsymbol{e}(t_f)]\| = 2.61e-6\ (m)$. Figure 6 shows that the input wrench constraints for the entire probability space were satisfied in a standard deviation sense. Figure 7 show that the specified terminal error variance was also satisfied, $\sigma^2_{e(t_f)} = 0.00321 \leq \overline{\sigma}^2_{e(t_f)} = 0.01\ (m^2)$.

The reduced power of the uncertain design, as compared to the deterministic design, makes sense in that the expected input wrench values, $E[\tau_1]$, of the uncertain design (as shown in Figure 6), are lower than those in the deterministic design (as shown in Figure 2). This relationship is also true for $\dot{q}_1$ (although are not illustrated), therefore, the product of the reduced expected torque and joint rate yields a lower system power.

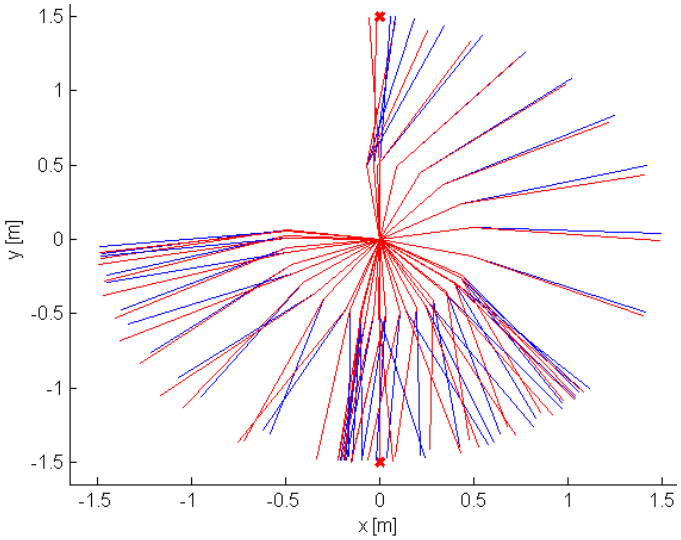

Figure 5—The *power optimal* configuration time history for the uncertain inverting double pendulum. This optimal solution resulted in a $310\ (W)$ design.

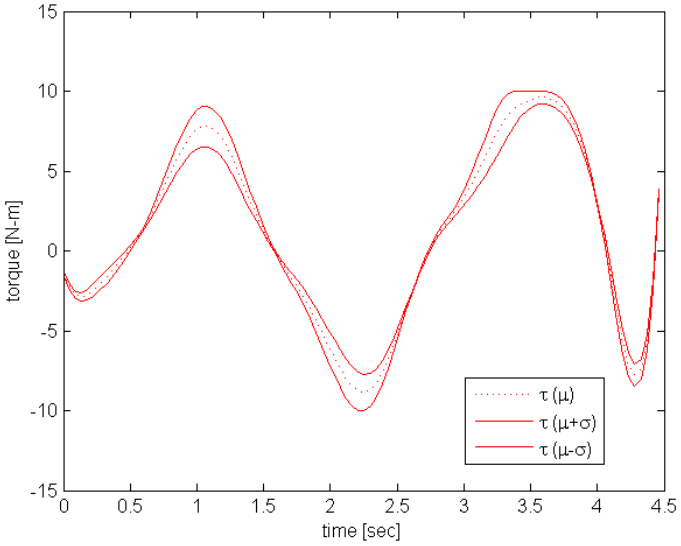

Figure 6—The uncertain input wrench time history resulting from the motion plan generated by the new uncertain optimal design framework. Both the maximum and minimum input limits were satisfied, in a standard deviation sense, for all systems within the probability space.

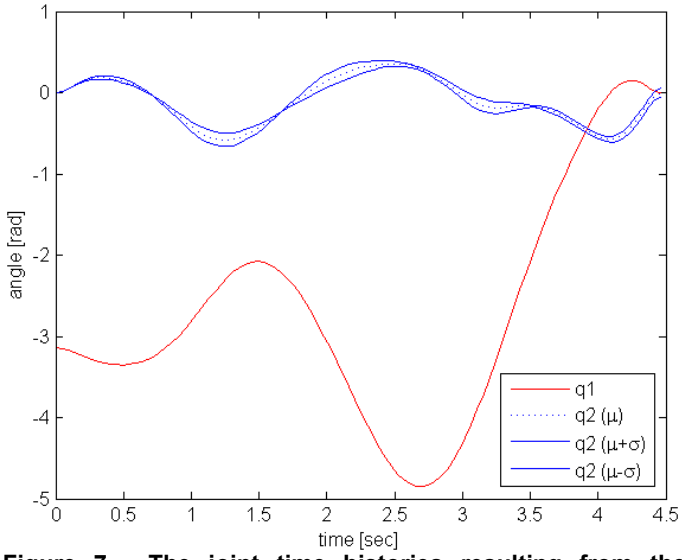

Figure 7— The joint time histories resulting from the motion plan generated by the new uncertain optimal design framework. The resulting terminal error variance satisfied the specification; $\sigma^2_{e(t_f)} = 0.0032 \leq \overline{\sigma}^2_{e(t_f)} = 0.01\ (m^2)$.

7 CONCLUSIONS

This work has presented a new nonlinear programming based motion planning framework that treats uncertain under-actuated dynamical systems. The framework allows practitioners to model sources of uncertainty using the Generalized Polynomial Chaos methodology and to solve the *uncertain hybrid dynamics* using a least-squares collocation method. Subsequently, statistical information of the *uncertain hybrid dynamics* may be included in the NLP's objective function and constraints. The inverting double pendulum case-study illustrated how the new framework produces an optimal design that accounts for the entire family of systems enabling a practitioner to design an optimally performing system that is also robust.

ACKNOWLEDGEMENTS

This work was partially supported by the Automotive Research Center (ARC), Thrust Area 1.

REFERENCES

[1] Hays, J., Sandu, A., Sandu, C., and Hong, D., 2011, "Motion Planning of Uncertain Fully-Actuated Dynamical Systems—an Inverse Dynamics Formulation," ASME IDETC/CIE Conference, Washington, DC, USA

[2] Hays, J., Sandu, A., Sandu, C., and Hong, D., 2011, "Motion Planning of Uncertain Fully-Actuated Dynamical Systems—a Forward Dynamics Formulation," ASME IDETC/CIE Conference, Washington, DC, USA

[3] Greenwood, D., 2003, *Advanced Dynamics*, Cambridge Univ Pr,

[4] Murray, R., Li, Z., Sastry, S., and Sastry, S., 1994, *A Mathematical Introduction to Robotic Manipulation*, CRC Press, Inc, Boca Raton, FL, USA.

[5] Nikravesh, P. E., 2004, Product Engineering, Springer, An Overview of Several Formulations for Multibody Dynamics.

[6] Haug, E. J., 1989, *Computer Aided Kinematics and Dynamics of Mechanical Systems. Vol. 1: Basic Methods*, Allyn & Bacon, Inc.,

[7] Lavalle, S., 2006, *Planning Algorithms*, Cambridge Univ Press, New York, NY, USA.

[8] Choset, H., 2005, *Principles of Robot Motion: Theory, Algorithms, and Implementation*, The MIT Press, Cambridge, MA, USA.
[9] Karaman, S., and Frazzoli, E., 2010 (submitted), "Incremental Sampling-Based Algorithms for Optimal Motion Planning," International Journal of Robotics Research, pp.
[10] Park, J., 2007, Industrial Robotics, Programming, Simulation and Applications, Verlag, Croatia, Optimal Motion Planning for Manipulator Arms Using Nonlinear Programming.
[11] Martin, B., and Bobrow, J., 1999, "Minimum-Effort Motions for Open-Chain Manipulators with Task-Dependent End-Effector Constraints," The International Journal of Robotics Research, 18 (2), pp. 213.
[12] Sohl, G. A., and Bobrow, J. E., 2001, "A Recursive Multibody Dynamics and Sensitivity Algorithm for Branched Kinematic Chains," Transactions of the ASME. Journal of Dynamic Systems, Measurement and Control, 123 (Copyright 2002, IEE), pp. 391-9.
[13] Bobrow, J. E., and Sohl, G. A., 2002, "On the Reliable Computation of Optimal Motions for Underactuated Manipulators," Electronic Journal of Computational Kinematics, 1 (1), pp.
[14] Bobrow, J., Martin, B., Sohl, G., Wang, E., Park, F., and Kim, J., 2001, "Optimal Robot Motions for Physical Criteria," Journal of Robotic systems, 18 (12), pp. 785-795.
[15] Sohl, G., 2000, "Optimal Dynamic Motion Planning for Underactuated Robots," PhD thesis, University of California, Irvine.
[16] Wang, C., Timoszyk, W., and Bobrow, J., 1999, "Weightlifting Motion Planning for a Puma 762 Robot," pp. 480-485.
[17] Wang, C., 2001, "Dynamic Motion Planning for Robot Manipulators Using B-Splines," thesis, University Of California,
[18] Xiang, Y., Arora, J., and Abdel-Malek, K., 2009, "Optimization-Based Motion Prediction of Mechanical Systems: Sensitivity Analysis," Structural and Multidisciplinary Optimization, 37 (6), pp. 595-608.
[19] Xiang, Y., Chung, H., Mathai, A., Rahmatalla, S., Kim, J., Marler, T., Beck, S., Yang, J., Arora, J., and Abdel-Malek, K., 2007, "Optimization-Based Dynamic Human Walking Prediction," Optimization, 1, pp. 2489.
[20] Chung, H., Xiang, Y., Mathai, A., Rahmatalla, S., Kim, J., Marler, T., Beck, S., Yang, J., Arora, J., and Abdel-Malek, K., 2007, "A Robust Formulation for Prediction of Human Running," pp. 16–18.
[21] Xiang, Y., Arora, J. S., Rahmatalla, S., and Abdel-Malek, K., 2009, "Optimization-Based Dynamic Human Walking Prediction: One Step Formulation," International Journal for Numerical Methods in Engineering, 79 (6), pp. 667-695.
[22] Xiang, Y., Chung, H.-J., Kim, J., Bhatt, R., Rahmatalla, S., Yang, J., Marler, T., Arora, J., and Abdel-Malek, K., 2010, "Predictive Dynamics: An Optimization-Based Novel Approach for Human Motion Simulation," Structural and Multidisciplinary Optimization, 41 (3), pp. 465-479.
[23] Xiang, Y., Arora, J., and Abdel-Malek, K., 2010, "Physics-Based Modeling and Simulation of Human Walking: A Review of Optimization-Based and Other Approaches," Structural and Multidisciplinary Optimization, 42 (1), pp. 1-23.
[24] Xiang, Y., 2008, "Optimization-Based Dynamic Human Walking Prediction," PhD thesis, University of Iowa, Iowa City, IA.
[25] Kim, H., Wang, Q., Rahmatalla, S., Swan, C., Arora, J., Abdel-Malek, K., and Assouline, J., 2008, "Dynamic Motion Planning of 3d Human Locomotion Using Gradient-Based Optimization," Journal of biomechanical engineering, 130, pp. 031002.
[26] Junggon, K., Jonghyun, B., and Park, F. C., 1999, "Newton-Type Algorithms for Robot Motion Optimization," Intelligent Robots and Systems, 1999. IROS '99. Proceedings. 1999 IEEE/RSJ International Conference on, 3, pp. 1842-1847 vol.3.
[27] Lee, S. H., Kim, J., Park, F. C., Kim, M., and Bobrow, J. E., 2005, "Newton-Type Algorithms for Dynamics-Based Robot Movement Optimization," Robotics, IEEE Transactions on, 21 (4), pp. 657-667.
[28] Featherstone, R., 2008, *Rigid Body Dynamics Algorithms*, Springer-Verlag New York Inc,
[29] Piegl, L. A., and Tiller, W., 1997, *The Nurbs Book*, Springer Verlag, Berlin, Germany.
[30] Wiener, N., 1938, "The Homogeneous Chaos," American Journal of Mathematics, 60 (4), pp. 897-936.
[31] Xiu, D., and Karniadakis, G., 2003, "The Wiener-Askey Polynomial Chaos for Stochastic Differential Equations," pp.
[32] Sandu, A., Sandu, C., and Ahmadian, M., 2006, "Modeling Multibody Systems with Uncertainties. Part I: Theoretical and Computational Aspects," Multibody System Dynamics, 15 (4), pp. 369-391.
[33] Sandu, C., Sandu, A., and Ahmadian, M., 2006, "Modeling Multibody Systems with Uncertainties. Part Ii: Numerical Applications," Multibody System Dynamics, 15 (3), pp. 241-262.
[34] Cheng, H., and Sandu, A., 2009, "Efficient Uncertainty Quantification with the Polynomial Chaos Method for Stiff Systems," Mathematics and Computers in Simulation, 79 (11), pp. 3278-3295.
[35] Xiu, D., and Hesthaven, J. S., 2005, "High-Order Collocation Methods for Differential Equations with Random Inputs," SIAM Journal on Scientific Computing, 27 (3), pp. 1118-1139.
[36] Xiu, D., 2007, "Efficient Collocational Approach for Parametric Uncertainty Analysis," Communications in Computational Physics, 2 (2), pp. 293-309.
[37] Xiu, D., 2009, "Fast Numerical Methods for Stochastic Computations: A Review," Communications in Computational Physics, 5 (2-4), pp. 242-272.
[38] Erdmann, M., 1984, "On Motion Planning with Uncertainty," Masters thesis, Massachusetts Institute of Technology, Boston.
[39] Barraquand, J., and Ferbach, P., 1995, "Motion Planning with Uncertainty: The Information Space Approach," International Conference on Robotics and Automation, 2, pp. 1341-1348.
[40] Park, W., Liu, Y., Zhou, Y., Moses, M., and Chirikjian, G., 2008, "Kinematic State Estimation and Motion Planning for Stochastic Nonholonomic Systems Using the Exponential Map," Robotica, 26 (04), pp. 419-434.
[41] Kewlani, G., Ishigami, G., and Iagnemma, K., 2009, "Stochastic Mobility-Based Path Planning in Uncertain Environments," pp. 1183-1189.